Water Research X 30 (2026) 100508

Contents lists available at ScienceDirect

Water Research X

journal homepage: www.sciencedirect.com/journal/water-research-x

Depth-partitioned nitrogen uptake sustained by ammonium in a nitrate-rich reservoir

Moyang Li [a], Xiaoyu Guo [a], Zifu Xu [b], Xianhui S. Wan [a], Lianghao Ge [a], Wenbin Zou [a], Jun Yang [c], Li-Li Han [b], Min Xu [b,*], Shuh-Ji Kao [b,*]

[a] State Key Laboratory of Marine Environmental Science, College of Ocean and Earth Sciences, Xiamen University, Xiamen, China
[b] State Key Laboratory of Marine Resource Utilization in South China Sea, Hainan University, Haikou, Hainan, China
[c] Aquatic Eco-Health Group, Fujian Key Laboratory of Watershed Ecology, State Key Laboratory of Regional and Urban Ecology, Institute of Urban Environment, Chinese Academy of Sciences, Xiamen, China

ARTICLE INFO

Keywords:
Eutrophication
Nitrogen uptake
Ammonium cycling
Heterotrophic processes
Niche separation

ABSTRACT

Thermal stratification in inland waters creates pronounced physicochemical gradients, yet a quantitative, depth-resolved understanding of how these gradients regulate nitrogen (N) dynamics remains lacking. Here, we conducted a two-year, depth-resolved study in a subtropical reservoir, quantifying uptake of ammonium (NH_4^+), nitrate (NO_3^-), and urea using the ^{15}N tracer labeling technique. Although NO_3^- is the dominant component of the dissolved inorganic nitrogen (DIN) pool in the euphotic zone, NH_4^+ consistently sustained the majority of N assimilation, exceeding NO_3^- and urea uptake by approximately 7- and 11-fold, respectively, resulting in rapid NH_4^+ turnover (median $\tau \approx 4$ days). Vertically, we observed a distinct three-layer structure of nitrogen assimilation along the light gradient: (1) phytoplankton preferentially utilized NH_4^+ and urea under high irradiance in the surface layer; (2) NO_3^- uptake peaked near the base of the euphotic zone, likely associated with low-light adapted diatoms; and (3) in the aphotic layer, substantial NH_4^+ assimilation persisted but decoupled from carbon fixation, indicating NH_4^+ consumption by heterotrophs. Our results provide a quantitative framework that refines our current view of nitrogen cycling in stratified inland waters and challenges concentration-based views of nutrient limitation. We demonstrate that effective management of eutrophication in stratified systems must account for N speciation, vertical stratification, and the distinct roles of autotrophic and heterotrophic communities.

1. Introduction

Inland waters play a key role in global biogeochemical cycles and carbon (C) burial (Mendonça et al., 2017). Their primary productivity and thus C sequestration potential are tightly coupled to nitrogen (N) cycling, which is increasingly perturbed by anthropogenic nutrient loading and climate change (Glibert, 2017; Zhang et al., 2025). While phosphorus (P) has traditionally been considered as the primary driver of eutrophication in freshwaters (Scavia et al., 2014), mounting evidence shows that combined N and P enrichment drives more severe phytoplankton blooms than P alone (Frost et al., 2023; Levine et al., 1997; Paerl et al., 2016). Among nitrogen species, ammonium (NH_4^+) is a key driver of productivity and bloom formation due to its high bioavailability and preferential uptake by phytoplankton (Raven et al., 1992). Nitrate (NO_3^-) is typically the most abundant DIN in oxygenated waters and serves as a complementary N source for phytoplankton. Meanwhile, urea, a reduced organic N form that is increasingly introduced via fertilizer application (Glibert et al., 2014), could also play an underappreciated role in phytoplankton productivity (Présing et al., 2001).

Much of our understanding of nitrogen dynamics in freshwater systems comes from shallow lakes, where only the surface layer is investigated, and these results highlight NH_4^+ dominance in assimilation (Ferber et al., 2004). Compared to shallow lakes, deep lakes or reservoirs exhibit pronounced vertical gradients in light and nutrients that create distinct microbial niches and nitrogen utilization patterns, yet these systems remain largely understudied (Li et al., 2025). For instance, although NO_3^- is usually a complementary N source at shallow depths, it becomes increasingly important at the lower euphotic zone due to the succession of the phytoplankton community (Wan et al., 2018). Moreover, heterotrophic microorganisms can contribute substantially to nitrogen cycling through NH_4^+ assimilation, highlighting the important

* Corresponding authors.
E-mail addresses: minxu@hainanu.edu.cn (M. Xu), sjkao@hainanu.edu.cn (S.-J. Kao).

https://doi.org/10.1016/j.wroa.2026.100508
Received 29 November 2025; Received in revised form 29 January 2026; Accepted 4 February 2026
Available online 5 February 2026

role of non-phototrophic processes in aquatic nitrogen dynamics (Kumar et al., 2008; Wheeler and Kirchman, 1986).

Although such vertical partitioning of nitrogen utilization has been conceptually recognized, its mechanistic implications remain poorly constrained because most freshwater nitrogen uptake studies have focused on shallow or weakly stratified systems, where vertical gradients are minimal and surface-layer measurements are often assumed to be representative of the entire water column. In deep, stratified reservoirs, however, the strong vertical segregation of light, nutrients, and oxygen may fundamentally reorganize nitrogen assimilation pathways across depth. Consequently, systematic, depth-resolved quantification of multiple nitrogen uptake pathways (NH_4^+, NO_3^-, and urea) remains rare in these systems, limiting our ability to generalize nitrogen cycling mechanisms and to predict ecosystem productivity and eutrophication dynamics in deep inland waters.

To address this gap, we conducted a two-year, depth-resolved investigation in a subtropical deep reservoir, combining vertical profiling with ^{15}N tracer experiments. By quantifying uptake rates of all major N forms across light gradients, we aimed to: (1) investigate seasonal variation of N composition and nitrogen assimilation in the seasonal stratified inland water; (2) uncover N source structure along the light gradient; (3) explore the potential mechanisms underpinning the vertical nitrogen assimilation pattern. The results are expected to provide new insights on nitrogen dynamics in the deep inland waters.

2. Method

2.1. Study site

The study was conducted in Shidou Reservoir (24°42′N, 118°00′E; **Supplementary Fig. S1**), a subtropical freshwater system situated in Xiamen, Fujian Province, southeastern China. This reservoir covers a surface area of 3.96 km^2, a catchment area of 67.37 km^2, and has a water residence time of ~370 days (Yang et al., 2016). During our study, water depth was ~18 m near the dam **(Supplementary Fig. S2)**, with fluctuations having negligible influence on the vertical structure at the sampling site. The reservoir exhibits typical lacustrine features, with a shallow euphotic zone (2–9 m, median = 5.5 m) overlying a deep aphotic zone. The euphotic layer deepens in summer relative to winter, while the pycnocline is located at ~4 m in spring and progressively deepens until complete mixing occurs in winter **(Supplementary Fig. S2)**.

The study area is characterized by a subtropical maritime monsoon climate with pronounced seasonality in precipitation and temperature, and with occasional typhoon events in summer and autumn. These climatic drivers lead to strong seasonal thermal stratification and marked vertical gradients in light, temperature, and nutrient availability. Stratified and mixed periods were identified using the relative thermal resistance to mixing (RTRM), with values >50 indicating stratification and <50 indicating mixing (Chimney et al., 2006; Wu et al., 2024; **Supplementary Text S1**). Additionally, parallel monitoring of dissolved inorganic phosphorus concentrations during the stratification period revealed generally low levels (< 0.2 μM) in the euphotic zone (data not shown).

2.2. Sample collection and incubation experiments

2.2.1. Experiment design

We conducted ten depth-resolved incubation experiments in 2022 and 2023, covering all seasons (January, April, June, August, October, and December in 2022; and March, June, September, and December in 2023). The incubations quantified multiple N uptake rates, including NH_4^+, NO_3^- and urea uptake, as well as ammonia urea oxidation. Uptake of C and nitrite (NO_2^-) was measured in selected experiments. Although ammonia oxidation data will be reported elsewhere, they were incorporated into calculations of DIN residence times (**Supplementary Text S2**). A full summary of experimental setups, including parameters, depth coverage, and light/dark treatments, is provided in **Supplementary Table S1**.

2.2.2. Water collection

Vertical profiles of temperature, salinity, and dissolved oxygen (DO) were obtained using an OCEAN SEVEN 316Plus CTD equipped with a DO sensor. Photosynthetically active radiation (PAR) was measured using a LI-COR underwater sensor, and chlorophyll fluorescence (Chl-a) was recorded using a Unilux fluorometer.

Water samples were collected at 1–2 m intervals using a Flow-jet pump and transferred into pre-rinsed 500 mL polycarbonate bottles. For each replicate, a volume of 50–200 mL of water was filtered through a GF/75 glass fiber filter (0.3 μm), adjusted based on filtration efficiency to prevent clogging. The filtrate was collected in acid-washed 50 mL centrifuge tubes (Falcon) for nutrient analysis, while the filters were preserved for particulate matter determination. All samples were collected in triplicate, immediately flash-frozen in liquid nitrogen, stored at −20 °C, and analyzed within three months.

For dissolved inorganic carbon (DIC), samples were collected in pre-combusted (450 °C, 4 h) 120 mL glass serum bottles, rinsed with in situ water and overfilled three times to minimize gas exchange. Bottles were sealed with 20 mm butyl rubber stoppers (Wheaton) and aluminum crimp caps, and preserved with 0.1 mL saturated $HgCl_2$. Samples were stored at 4 °C and analyzed within one month.

2.2.3. Incubation setup

The euphotic zone was defined as the depth of 1% surface PAR (sPAR). Incubation experiments were performed at three standard depths within the euphotic zone (100%, 10%, and 1% sPAR), with each depth incubated under paired light and dark treatments. Below the euphotic zone, incubations were conducted at 2–5 depths under dark conditions. In June, September, and December 2023, paired light/dark incubations were also conducted at 0.1% sPAR. Depths were determined by CTD-derived PAR profiles on each sampling date. Target light intensities were calculated by applying attenuation coefficients to MODIS-derived monthly mean sPAR **(Supplementary Fig. S3)**. Light intensity was not measured in December 2022, therefore, the irradiance was estimated using the December 2021 PAR profile.

All incubation experiments were performed in temperature-controlled incubators set to near in situ temperature, and an artificial sunlight system was used to mimic in situ light intensity (Hydra® 64HD, AquaIllumination). Water for incubations was collected in 20 L acid-washed, light-shielded containers and transported to the laboratory, with incubations initiated within 5 h of sample collection in most cases. Subsamples were transferred into pre-rinsed 250 mL polycarbonate Nalgene bottles. For each rate measurement, triplicate bottles were sampled at three time points ($n = 9$). Incubation durations ranged from 3 to 16 h with light incubations restricted to ≤12 h **(Supplementary Table S1)**.

In addition to the depth-resolved incubations, additional sets of experiments were conducted to evaluate substrate kinetics and temperature dependence. Haldane inhibition uptake kinetics for NH_4^+ and Michaelis–Menten kinetics for urea were determined in dark incubations using five substrate concentrations, conducted at 7 m in August 2022 and at 4 m in March 2023, respectively. To examine the effect of temperature on NH_4^+ uptake, a series of dark incubations was carried out at 13 m in December 2022 under six temperature treatments.

Tracers were added as 0.2 mL aliquots: $^{15}NH_4Cl$ (99 atom% ^{15}N), $K^{15}NO_3$ (99 atom% ^{15}N), ^{15}N-urea (98 atom% ^{15}N), $Na^{15}NO_2$ (98 atom% ^{15}N), or $NaH^{13}CO_3$ (99 atom% ^{13}C), all from Cambridge Isotope Laboratories. Tracer enrichments were adjusted according to ambient concentrations at each depth. Final average tracer enrichments (% of the ambient substrate pool) were: $^{15}NH_4^+$: 16 ± 15%, $^{15}NO_3^-$: 10 ± 9%, ^{15}N-urea: 40 ± 30%, $^{15}NO_2^-$: 14 ± 3%, and ^{13}C: 6 ± 2% **(Supplementary Table S1)**.

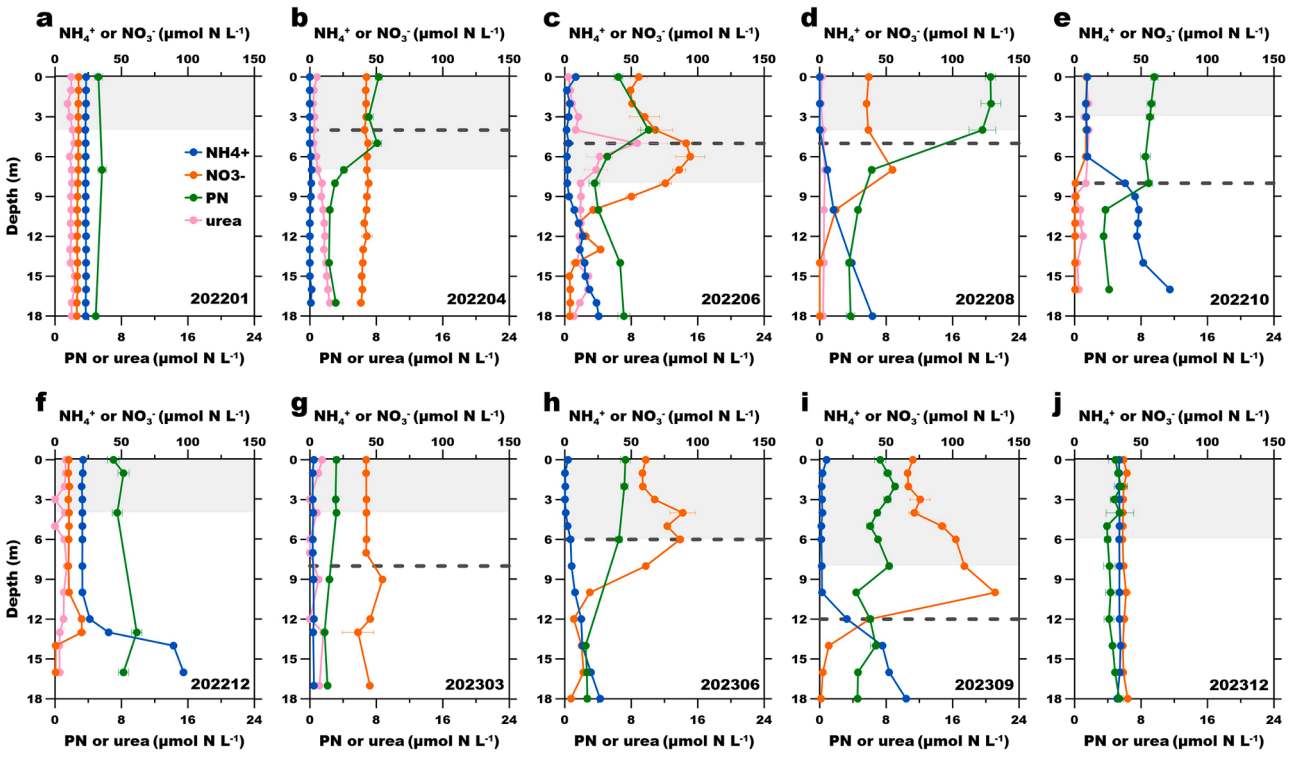

Fig. 1. Vertical profiles of N species throughout the sampling period. Blue, orange, green and pink dotted lines represent NH_4^+, NO_3^-, PN and urea concentrations, respectively. Data are presented as mean ± standard deviation (SD) of triplicate samples; error bars are smaller than symbols where not visible. The grey area represents the euphotic zone. The dashed lines mark the depth of the pycnocline during stratified periods.

To quantify nitrogen uptake under environmentally relevant conditions, we adopted a non-saturating tracer approach that has been widely applied in aquatic studies (Baer et al., 2017; Wan et al., 2021). Unlabeled substrate (2.5 μM final concentration) was therefore added during euphotic zone incubations (NH_4^+ in April, June, August 2022, and June 2023; urea in June and August 2022) to prevent substrate depletion during incubation while minimizing perturbation to ambient substrate regimes. In December 2023, a 5 μM $^{14}NO_2^-$ carrier was added at the surface to represent a potential rate condition. Immediately following tracer addition, t_0 whole-water samples, including both particulate and dissolved phases, were filtered and the filtrate was split into three aliquots per replicate to minimize freeze–thaw cycles for subsequent nutrient and isotope analyses.

2.3. Chemical measurements

Concentrations of DIN were determined with a four-channel Auto-Analyzer (Bran+Luebbe Co., Germany). Detection limits were 0.07 μmol L^{-1} for NO_x^- ($NO_3^- + NO_2^-$) and 0.14 μmol L^{-1} for NH_4^+. Urea concentrations were determined colorimetrically using the diacetylmonoxime method with a 5 cm pathlength cell, achieving a detection limit of 40 nmol N L^{-1} (Revilla et al., 2005).

DIC was measured by quantifying CO_2 released upon acidification, using a non-dispersive infrared detector (Li-Cor® 7000) coupled to an Apollo SciTech AS-C6 DIC Analyzer, with a precision of ±2 μmol kg^{-1}.

Particulate nitrogen (PN) concentrations were determined by oxidizing freeze-dried filters to NO_3^- using purified persulfate as an oxidizing reagent (Knapp et al., 2005), followed by quantification of NO_3^- via chemiluminescence (Braman and Hendrix, 1989). Filters were digested in 12 mL pre-combusted (450 °C, 4 h) borosilicate tubes with 1 mL purified persulfate oxidizing reagent (POR; Merck, ACS-grade; recrystallized ≥3 times) and 5 mL deionized water, then autoclaved at 120 °C for 1 h. The chemiluminescence method had a detection range of 0.1–20 μmol L^{-1} (PN equivalent) and a precision of 2%. Procedural blanks included POR-only tubes ($n \geq 6$) and unused pre-combusted filters.

Particulate organic carbon (POC) was measured by freeze-drying filters, acidifying with 1 mL of 1 N HCl to remove carbonates, drying at 50 °C for 48 h, and analyzing with an EA-IRMS (vario PYRO Cube interfaced to an IsoPrime 100 isotope ratio mass spectrometer). Acetanilide (Merck, C% = 71.09) served as the concentration standard and was run every 10 samples. The analytical precision for POC concentration was <1% (Kao et al., 2012).

2.4. Isotopic analyses

The $\delta^{15}N$ of NO_x^- was determined using the denitrifier method (Sigman et al., 2001; Casciotti et al., 2002). Briefly, NO_x^- was quantitatively converted to N_2O using the *Pseudomonas aureofaciens* (ATCC No 13985), which was cryogenically purified and introduced into a Thermo Finnigan Gasbench-IRMS (Delta V Advantage). Calibration utilized international standards (USGS-34, $\delta^{15}N = 1.8‰$; IAEA-N-3, $\delta^{15}N = 4.7‰$; USGS-32, $\delta^{15}N = 180.0‰$) supplemented by an in-house standard ($\delta^{15}N = 13.8‰$), analyzed before and after every 10 samples. Accuracy (pooled standard deviation) was better than ± 0.2‰ according to analyses of these standards at an injection level of 20 nmol N.

The $\delta^{15}N$ of PN was determined from the digested samples using the same denitrifier-IRMS protocol. PN concentration and $\delta^{15}N$ were corrected for POR blanks (typically <2% of total N) and filter blanks (1.50 ± 2.08 nmol N).

The $\delta^{13}C$ of POC was determined alongside POC concentration by EA-IRMS, calibrated with international standards (USGS-40, $\delta^{13}C = -26.24‰$; USGS-41, $\delta^{13}C = 36.55‰$; IAEA-600, $\delta^{13}C = -27.5‰$). Standards were analyzed every 10 samples to ensure accuracy.

2.5. Rate calculations

Reaction rates were calculated based on the accumulation of ^{15}N in

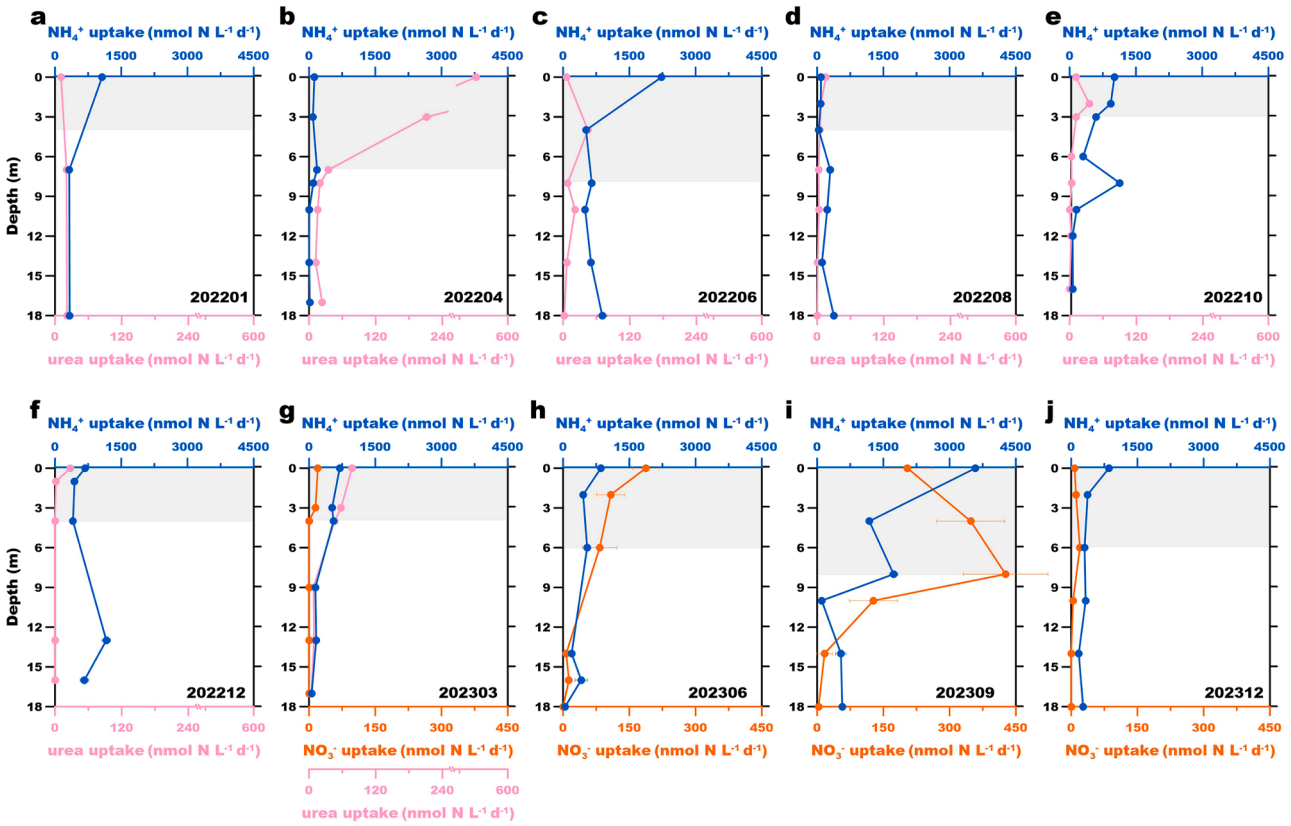

Fig. 2. Vertical profiles of N uptake rates across the sampling period. Blue, pink, and orange dotted lines represent NH_4^+, urea, and NO_3^- uptake rates, respectively. The grey area represents the euphotic zone. Data are presented as mean ± SD of triplicate samples; error bars are smaller than symbols where not visible.

the product pool relative to t_0 samples. Uptake and oxidation rates were calculated using Eqs. (1) and (2):

$$R_{bulk} = \frac{C_t \times n_t - C_0 \times n_0}{t \times f^{15}} \quad (1)$$

$$R_{in-situ} = R_{bulk} \times \frac{Ci_s}{Ci_s + Ct_s} \quad (2)$$

where R_{bulk} is the bulk reaction rate (nmol N L^{-1} h^{-1}); C_t and C_0 are product concentrations at the end and start of the incubation (nmol N L^{-1}); n_t and n_0 are atom% ^{15}N of the product pool at the end and beginning of the incubation, respectively; f^{15} is the atom% ^{15}N of the substrate pool at the start of the incubation; t is the incubation duration (h); $R_{in-situ}$ is the in situ reaction rate calibrated by linear interpolation; and Ci_s and Ct_s represent the initial substrate and final tracer concentrations, respectively. For nutrient concentrations below detection, half the detection limit was used in calculations. Rates were derived from linear regressions of product accumulation across the three time points for each incubation. In most cases, the accumulation of ^{15}N-labeled products was well approximated by linear functions (typically $R^2 > 0.9$), indicating that incubations remained close to steady state over the experimental period.

Daily gross uptake rates were estimated as:

$$\text{Daily rate} = \text{Light rate} \times \text{Day length} + \text{Dark rate} \times \text{Night length} \quad (3)$$

with day length derived from sunrise/sunset times based on sampling date and site coordinates (https://github.com/beaudu/sunrise).

We quantified the light effect (light-induced enhancement %) as the relative increase in uptake rate under light compared to dark conditions, calculated as:

$$\text{Light} - \text{induced enhancement \%} = \frac{R_{light} - R_{dark}}{R_{dark}} \times 100\% \quad (4)$$

Further details on the calculations for Haldane inhibition kinetics, Michaelis-Menten kinetics, Q_{10} temperature coefficient, relative N preference index (RPI), and DIN residence times are provided in **Supplementary Text S2**.

3. Result

3.1. Vertical distribution of nitrogen across seasons

The subtropical reservoir (Shidou Reservoir) exhibited pronounced seasonal stratification during the warm months and was well-mixed in winter, resulting in marked changes in DO, Chl-a, and nutrient profiles (Fig. 1; **Supplementary Fig. S4)**. Across the ten surveys, DIN species displayed distinct vertical segregation. In the euphotic zone, NO_3^- predominated (8.7–108.9 μM; mean = 47.9 μM), while NH_4^+ was relatively low (below detection to 33.8 μM; mean = 9.3 μM). Below this layer, NH_4^+ accumulated up to 96.7 μM, whereas NO_3^- often declined to undetectable levels, with occasional subsurface maxima near the base of the euphotic zone (Fig. 1). Winter mixing erased these vertical gradients, yielding vertically uniform NH_4^+ and NO_3^- profiles (Fig. 1a, j). Urea concentrations were consistently low (<2 μM), except for a single peak of 4.4 μM observed in the euphotic zone in June 2022 (Fig. 1c). PN concentrations were higher in the euphotic zone (average: 7.6 μM; range: 3.1–20.6 μM) than in the aphotic zone (average: 4.6 μM; range: 1.8–9.8 μM), reflecting phytoplankton biomass distribution (Fig. 1). Overall, these patterns demonstrated that physical stratification not only controls vertical nutrient segregation but also regulated the balance between oxidized and reduced N forms, with implications for nitrogen form availability to

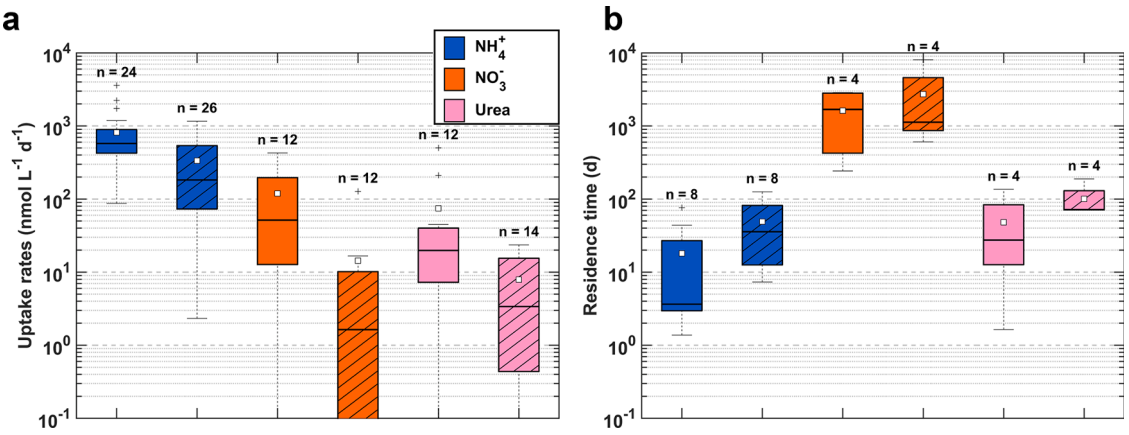

Fig. 3. Distribution of uptake rates and residence times between euphotic and aphotic zones. Blue, orange, and pink indicate NH_4^+, NO_3^-, and urea groups, respectively. Solid boxes without and with diagonal hatching represent the euphotic and aphotic zones, respectively, and black lines and white squares denote medians and means.

distinct microbial communities across the depth and season.

3.2. Various nitrogen species uptake and residence time

N uptake rates displayed a typical vertical gradient, with higher values located in the euphotic zone accompanied with a sharp decline below (Fig. 2). NO_3^- and urea uptake both dropped steeply beneath the euphotic zone, frequently falling below detection limits. In contrast, substantial NH_4^+ uptake was consistently observed in the aphotic zone (Fig. 2; Fig. 3a; **Supplementary Fig. S5**).

NH_4^+ uptake exhibited pronounced seasonal variability, generally showing highest rates in surface waters during summer and autumn, with a peak of 3585.2 nM N L^{-1} d^{-1} recorded in September 2023. However, rates were occasionally low, likely due to nutrient limitation (Fig. 1d), such as the 88.4 nM N L^{-1} d^{-1} observed in August 2022 (Fig. 2d). During winter, NH_4^+ uptake was lower than that in summer and autumn, but was comparable to spring values and became vertically homogeneous (Fig. 2a, f, j).

NO_3^- uptake also increased during summer and autumn, reaching a maximum rate of 426.7 nM N L^{-1} d^{-1} in the surface layer in September 2023. Urea uptake remained relatively low throughout the year. However, the highest urea uptake rate observed in April 2022 reached 501.1 nM N L^{-1} d^{-1}. Except for this single observation, the rates were always lower than 80 nM N L^{-1} d^{-1}. Additionally, all attempts to measure NO_2^- uptake consistently resulted in values below detection limits, indicating negligible NO_2^- uptake in this system.

Across all measurements, NH_4^+ uptake in the euphotic zone (average: 812.9; median: 575.0 nM N L^{-1} d^{-1}) exceeded NO_3^- uptake (average: 119.2; median: 51.4 nM N L^{-1} d^{-1}) by ~7-fold and urea uptake (average: 74.6; median: 19.8 nM N L^{-1} d^{-1}) by ~11-fold (Fig. 3a). This dominance of NH_4^+ uptake became even more pronounced in the aphotic zone, where NH_4^+ uptake exceeded NO_3^- and urea uptake by approximately 23- and 42-fold, respectively.

The residence time further underscored rapid NH_4^+ turnover (median $\tau = 4$ days), compared to slower cycling of urea (27 days) and NO_3^- (1683 days) in the euphotic zone (Fig. 3b). This pattern also held in the aphotic zone, where NH_4^+, urea, and NO_3^- had median residence times of 36, 71, and 1126 days, respectively. However, the actual residence time of NO_3^- in the aphotic zone is likely shorter due to denitrification losses. These differences suggest that NH_4^+ serves as the dominant, rapidly recycled N source for microbial communities, whereas NO_3^- and urea represent complementary N sources and exhibit slower turnover rates.

During the stratified period, nitrate concentrations in the euphotic zone exceeded NH_4^+ by nearly two orders of magnitude. For example, in June 2023 the mean concentrations of NH_4^+ and NO_3^- were 1.47 μM and 71.45 μM, respectively. Surprisingly, NH_4^+ uptake rates still surpassed those of NO_3^-. This decoupling from concentration dependence indicates a strong physiological preference for NH_4^+ by phytoplankton **(Supplementary Fig. S6)**, probably due to the lower energetic cost of utilizing NH_4^+ compared to other N forms.

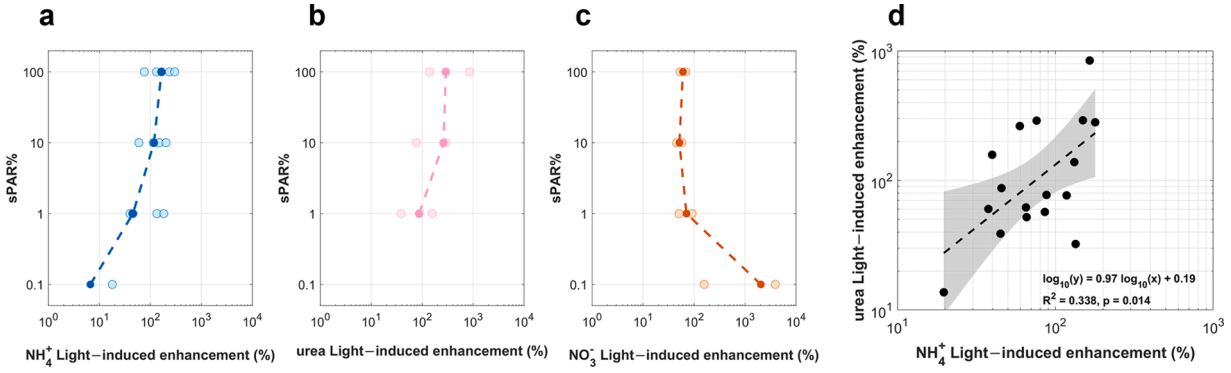

Fig. 4. Light effect (light-induced enhancement) on NH_4^+, urea, and NO_3^- uptake. (a-c) light effect on NH_4^+, urea and NO_3^- uptake under 100%, 10%, 1% and 0.1% sPAR incubations during summer and autumn (June, August, and October in 2022; June and September in 2023). Light colored circles represent individual measurements, and dark colored circles show median values for each sPAR group, connected by dashed lines. (d) Linear regression of NH_4^+ and urea light effects in log scale. Shaded area indicates the 95% confidence interval.

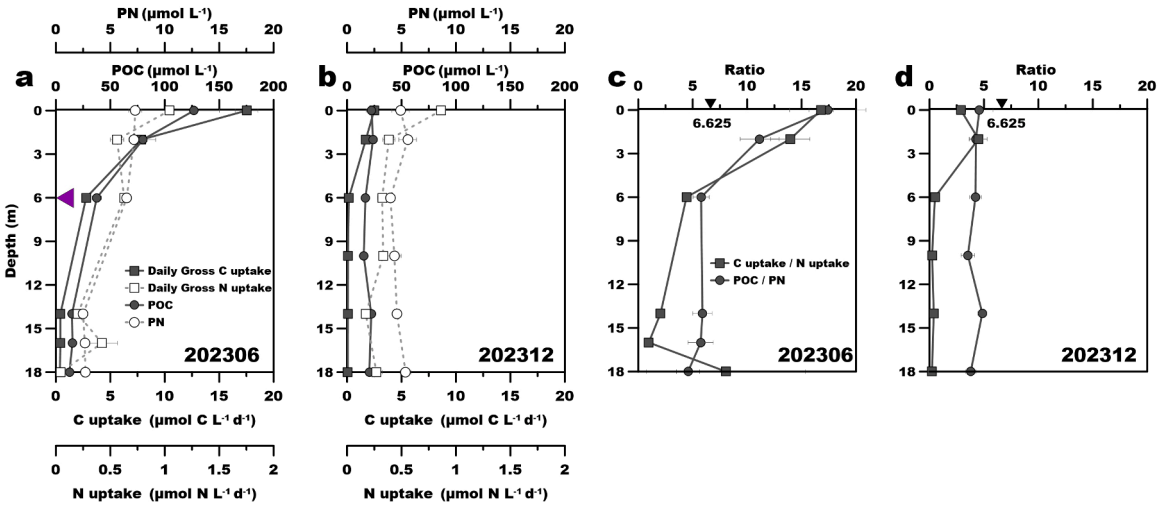

Fig. 5. C and N uptake dynamics and stoichiometric relationship. (a,b) Vertical profiles of C and N uptake rates and POC and PN. Open and solid gray squares depict C and N uptake rates (nmol C L^{-1} h^{-1}) and open and solid gray circles depict POC and PN. (c,d) Ratios of C:N uptake rates versus POC:PN ratios. Solid gray squares and circles lines represent C:N uptake rates and POC:PN, respectively. For all four subgraph N uptake represent the sum of NH_4^+ and NO_3^- uptake, considering the data matching and the negligible uptake of urea in summer and winter. Error bars represent ± SD of triplicate measurements. Purple triangles indicate the depth of the euphotic zone (6 m in both June and December). Black triangles indicate the Redfield ratio.

3.3. Vertical partitioning of nitrogen utilization strategies and light-induced enhancement in euphotic zone

Light is a fundamental determinant of phytoplankton activity, and different responses to irradiance among taxa can lead to vertical niche partitioning in nitrogen utilization. In our study, the stimulatory effect of light on NH_4^+ uptake generally declined with depth (Fig. 4a), indicating dominance of high light adapted phytoplankton. An exception occurred in spring 2022, when the opposite pattern was observed, whereas in spring 2023 the typical pattern reappeared **(Supplementary Fig. S7a, p)**. Although the mechanism remains uncertain, stronger N limitation in the euphotic zone during spring 2022 may have contributed to this anomaly. Additionally, concurrent light/dark incubations at the 0.1% sPAR depth in June, September, and December 2023 revealed negligible light stimulation of NH_4^+ uptake **(Supplementary Fig. S7q–s)**, suggesting that assimilation at this depth was dominated by heterotrophs whose activity is largely decoupled from irradiance. Moreover, the co-variation in light effects on NH_4^+ and urea uptake across all seasons and depth suggested assimilation of these N species by similar plankton functional groups (Fig. 4a, b, d).

In contrast, NO_3^- uptake often exhibited subsurface maxima in its light response (Fig. 4c **Supplementary Fig. S7i–o**). Although only one profile (September 2023) showed a pronounced subsurface peak in NO_3^- uptake rates (Fig. 2i), corresponding to the highest productivity period of the two-year study, strongly supporting the robustness of this signal. Additional evidence was observed in winter 2023, when NO_3^- uptake reached its maximum near the base of the euphotic zone. During peak productivity in September 2023, the NO_3^- uptake rate at 0.1% sPAR depth even surpassed NH_4^+ uptake at the same depth, which was the only instance recorded. Although the NO_3^- uptake peak was slightly shallower than the depth of maximum light response, both peaks occurred in the subsurface layer **(Supplementary Fig. S7i)**. Combined with the predominance of NH_4^+ uptake in surface waters, these vertical patterns provide strong evidence for niche differentiation among nitrogen assimilators.

Previous studies have found that cyanobacteria preferentially utilize NH_4^+, whereas diatoms exhibit a preference for NO_3^- (Glibert et al., 2016). Consistent with a possible interpretation of these uptake patterns, previous studies conducted in Shidou Reservoir have reported that Cyanobacteria, Bacillariophyta (diatoms), and Chlorophyta constitute the dominant phytoplankton groups, with cyanobacteria being particularly abundant in surface waters (Liu et al., 2019; Yang et al., 2017). The observed decline in microcystin concentrations with depth in summer (Xue et al., 2024) indicates a reduced relative contribution of cyanobacteria at greater depths, which is qualitatively consistent with the vertical pattern of NH_4^+ uptake observed here.

Collectively, these results suggest that light availability plays a pivotal role in structuring phytoplankton communities and their vertical nitrogen utilization strategies, ultimately influencing water column productivity and C export. For instance, when certain groups with high sinking potential, such as diatoms taxa, are positioned deeper in the water column, their contribution to export may be enhanced due to both their intrinsic particle properties and spatial proximity to the sediment interface.

3.4. Ammonium assimilation by heterotrophs decouples nitrogen from carbon cycling in aphotic zone

Below the euphotic zone, C uptake declined sharply, mirroring the decrease in NO_3^- and urea uptake, but contrasted with the sustained NH_4^+ uptake observed in the aphotic zone (Fig. 5a, b). Notably, the C:N uptake ratio in these dark waters deviated markedly from the ambient POC:PN ratio (Fig. 5c, d), suggesting that heterotrophic microorganisms assimilated NH_4^+ with minimal concurrent DIC uptake. Such decoupling pattern has also been reported in Lake Superior (Kumar et al., 2008). In addition, vertical profiles from June 2023 showed concurrent declines in POC and PN with depth, while isotopic signatures of particulate matter exhibited pronounced ^{15}N enrichment below the euphotic zone **(Supplementary Fig. S8a)**. These lines of evidence point to active heterotrophic microbial degradation of organic matter in the aphotic zone. While oxygen exposure during sample handling may slightly elevate absolute NH_4^+ uptake rates in the aphotic zone, this bias would uniformly affect all depths and nitrogen forms. Importantly, the dominance of NH_4^+uptake over NO_3^- and urea persists throughout the entire water column and across all sampling periods, including in winter. These consistencies indicate that the observed vertical pattern reflects a real and robust feature of nitrogen cycling rather than a methodological artifact.

Depth-weighted uptake rates showed that NH_4^+ assimilation in the aphotic zone reached a median of 41% of the euphotic zone rate (euphotic:aphotic uptake ratio = 2.43; **Supplementary Fig. S5a)**. These depth-weighted and depth-integrated comparisons are intended to

provide a system-level contrast between euphotic and aphotic nitrogen uptake, rather than a quantitative separation of biological pathways. Likewise, depth-integrated estimates indicated that NH_4^+ uptake in the aphotic zone accounted for 54% of NH_4^+ assimilation in the euphotic zone (euphotic:aphotic uptake ratio = 1.86; **Supplementary Fig. S5c)**. Together, these findings underscore the substantial role of heterotrophic communities in sustaining nitrogen assimilation in dark waters, thereby extending the active N uptake to the aphotic zone.

4. Discussion

4.1. Ammonium dominates nitrogen assimilation

Similar patterns of NH_4^+-dominated N assimilation have been observed in other surface waters (Ferber et al., 2004; Kumar et al., 2008), though elevated urea can occasionally become dominant (Présing et al., 2001). In contrast, higher NO_3^- uptake than NH_4^+ in Sandusky Bay under high ambient NO_3^- levels was reported (Salk et al., 2018). Upon closer examination, we found their DIN uptake results exhibited spatial variability: in upstream regions with low N:P ratios (<16), NO_3^- uptake exceeded NH_4^+ uptake, likely reflecting substrate-driven assimilation under N-limited conditions. However, in downstream regions with elevated NO_3^- concentrations and much higher N:P ratios (often >100), NH_4^+ uptake dominated. This suggests that in more hydrologically stable waters, which are typically characterized by P limitation, phytoplankton preferentially assimilate NH_4^+ despite abundant NO_3^- availability, consistent with our observations. Importantly, these findings underscore that nitrogen assimilation pathways are not solely determined by bulk nutrient concentrations, but are strongly modulated by nutrient stoichiometry, hydrodynamic stability, and associated ecological niches.

Preferential uptake of NH_4^+ under NO_3^--replete conditions has been widely documented across diverse aquatic ecosystems (Baer et al., 2017; Kumar et al., 2008). This preference is commonly attributed to the lower energetic cost of NH_4^+ uptake and assimilation, as well as its more efficient transport across cell membranes (Glibert et al., 2016). As a result, NH_4^+ often dominates nitrogen assimilation despite representing only a minor fraction of the dissolved inorganic nitrogen pool.

Direct quantitative comparisons with other subtropical and temperate reservoirs remain limited, largely because most freshwater nitrogen uptake studies have focused on shallow or weakly stratified systems, where vertical gradients are weak and depth-integrated measurements may obscure vertically structured processes. Consequently, depth-resolved assessments of multiple nitrogen uptake pathways in deep, stratified reservoirs are still rare. Rather than extrapolating absolute uptake rates across systems, our results highlight a generalizable mechanistic pattern: stratification-driven vertical organization of nitrogen assimilation, with NH_4^+ dominating uptake throughout the water column, NO_3^- uptake becoming relatively more important near the base of the euphotic zone, and substantial NH_4^+ assimilation persisting in aphotic waters via heterotrophic processes.

4.2. Contributions of heterotrophs in the euphotic zone

N uptake was also detectable in dark incubations in the euphotic zone, particularly for NH_4^+, suggesting contributions from heterotrophic microbes and/or light-independent uptake by phytoplankton. Previous studies have shown that heterotrophic microorganisms can effectively compete with phytoplankton for inorganic nitrogen substrates under nutrient-limited conditions (Joint et al., 2002; Deng et al., 2021; Wheeler and Kirchman 1986), and that the availability of photosynthetically derived labile organic matter can further stimulate heterotrophic metabolism. These observations collectively suggest that heterotrophs may play a significant role in nitrogen assimilation in surface waters.

The difference between light and dark incubations provides a useful constraint on light-dependent versus light-independent nitrogen uptake, but it should be interpreted cautiously. Dark incubations represent an upper bound on heterotrophic uptake, because phytoplankton are known to maintain NH_4^+ assimilation for several hours in the absence of light. Consequently, light–dark contrasts cannot be used to derive a strict quantitative partitioning between autotrophic and heterotrophic processes. Using this approach, the average light-induced enhancement of 133% (Fig. 4a) corresponds to a light: dark uptake ratio of 2.33, which would imply that processes other than light-dependent autotrophy (i.e., heterotrophy and dark phytoplankton uptake) could account for up to ~30% of total NH_4^+ assimilation in the euphotic zone. This fraction is ecologically significant, as it indicates that a substantial portion of NH_4^+ assimilation in surface waters is supported by light-independent processes. This result highlights that heterotrophic uptake represents a non-negligible component of nitrogen cycling even within the euphotic zone. While our experimental design cannot fully partition the different sources of dark N uptake, its consistent detection indicates that heterotrophic processes operate alongside autotrophic activity in the euphotic zone and contribute meaningfully to nitrogen cycling. Evidence from other ecosystems has revealed even more striking patterns, where dark uptake rates exceeded those under light incubation (Sepp et al., 2025).

Seasonal patterns further illustrate the interplay between autotrophic and heterotrophic processes. During the stratified period of 2023, both C and N uptake, as well as POC and PN concentrations, peaked at the surface and declined with depth, reflecting intense primary production in the upper water column and net remineralization below. In contrast, winter mixing produced more homogeneous vertical profiles (Fig. 5a, b), indicative of substrate redistribution and a more vertically uniform distribution of microbial activity.

Particulate stoichiometry provides additional insight. The close correspondence between C:N uptake ratios and POC:PN ratios (Fig. 5c, d) suggests tight coupling of organic matter production and degradation. However, in June 2023, the C:N uptake ratio reached 17.4, well above the Redfield ratio. Such anomalies are unusual, though occasionally observed in nutrient-limited systems (Kumar et al., 2008; Henderson et al., 2025). Despite high DIN concentrations, assimilation was constrained by the low availability of NH_4^+ **(Supplementary Fig. S8c)**, which is the preferred substrate. NO_3^- uptake rates were much lower, so the high NO_3^- concentration effectively masked the N form most relevant to phytoplankton demand. Under these conditions, N limitation promotes the production of C-rich extracellular material and enhances heterotrophic decomposition of organic N, leaving residues enriched in carbon. The elevated $\delta^{13}C$ values of POC (−24‰) observed in June further support this interpretation. Rather than merely indicating high productivity, this isotopic enrichment aligns with enhanced heterotrophic respiration, which preferentially removes ^{12}C and leaves residual POC enriched in $\delta^{13}C$ and carbon (Lehmann et al., 2004). These stoichiometric and isotopic signals independently corroborate a substantial heterotrophic presence in the euphotic zone, consistent with the dark-incubation evidence described above.

The present study focuses on process-level nitrogen uptake patterns derived from tracer incubations. While depth-dependent variations in biological communities are likely to contribute to the observed vertical structure, the current analysis does not include depth-resolved community composition data that can be directly linked to individual uptake measurements. Consequently, the interpretation of uptake patterns is framed at the functional level, and any association with specific biological groups should be considered indicative rather than definitive.

4.3. Environmental control of nitrogen uptake

The observation of Haldane inhibition kinetics for NH_4^+ uptake at 7 m (August 2022), combined with weak light response at 0.1% sPAR (Fig. 4a), indicates minimal photoautotrophic contribution below the euphotic zone. This depth also coincided with a sharp decline in PN

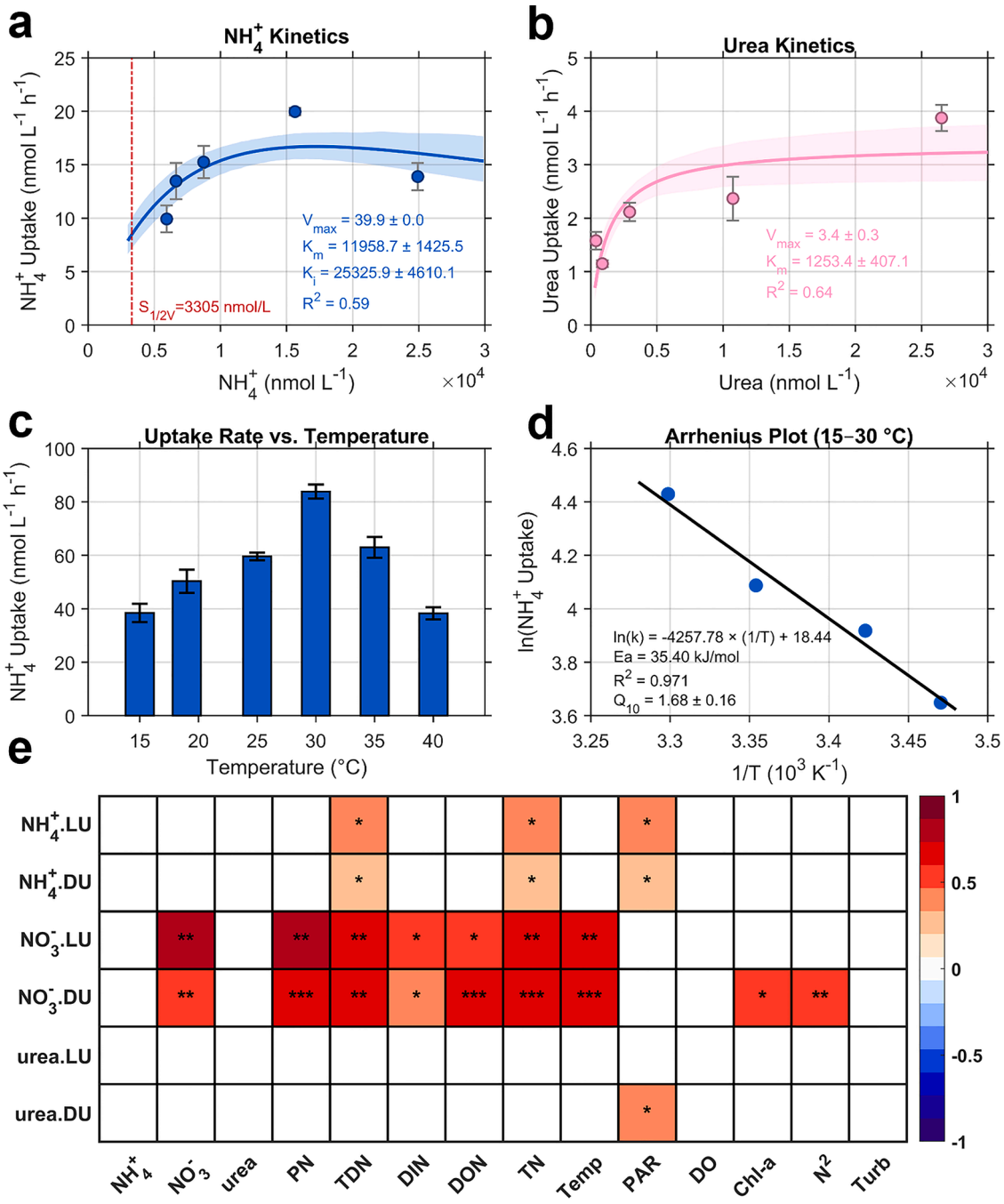

Fig. 6. Environmental drives of N uptake kinetics. (a) NH_4^+ uptake kinetics fitted with the Haldane substrate inhibition model. The red dashed vertical line indicates $S_{1/2V}$, the substrate concentration at half of the modeled peak uptake rate. (b) Michaelis-Menten kinetics for urea uptake. (c,d) Temperature response of NH_4^+ uptake and Arrhenius plot between 15–30°C. (e) Pearson correlation matrix for key parameters. The color gradient denotes correlation coefficients; only significant correlations ($P < 0.05$, two-sided) are colored (white squares: $p > 0.05$). Significance levels: ***$P < 0.001$, **$P < 0.01$, *$P < 0.05$. LU and DU denote light and dark uptake rates, respectively.

(Fig. 1), suggesting active remineralization. The mid-water NH_4^+ uptake peak likely reflects heterotrophic activity. The substrate concentration required to reach half of the observed peak rate ($S_{1/2\ V} \approx 3$ μM) is comparable to the half-saturation concentrations reported for other lake and ocean environments (Gu and Alexander, 1993; Xu et al., 2019). Subsurface urea uptake followed Michaelis-Menten kinetics (Fig. 6b), showing concentration-dependent stimulation. Given the low ambient urea levels in the reservoir (0.08–1.5 μM), even modest increases may substantially elevate urea uptake.

Temperature response assays at 13 m (December 2022) revealed increasing uptake rate up to 30 °C (Fig. 6c, d), with a Q_{10} of 1.68, slightly below the typical 2–4 range. According to the annual temperature range at this depth (15.9–24.3 °C), warming likely enhances NH_4^+ uptake in mid-depth waters.

Although NO_3^- uptake exhibited significant correlations with several environmental variables (Fig. 6e), this does not diminish the ecological relevance of NH_4^+ in this system. Instead, it highlights a fundamental distinction between state variables and process variables. NO_3^-, with its large and relatively stable pool, responds coherently to physical and chemical gradients and therefore shows strong statistical associations with temperature, stratification, and nutrient inventories. In contrast, NH_4^+ functions as a rapidly recycled, low-concentration flux, whose

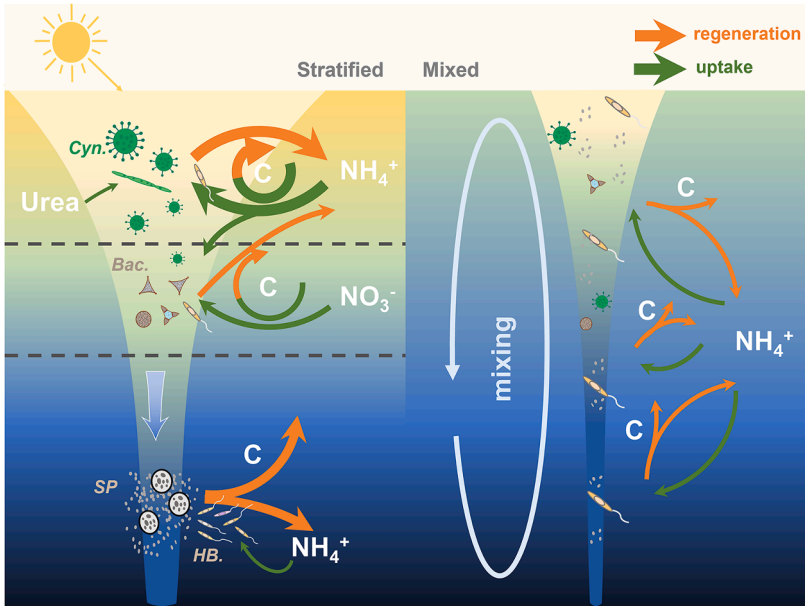

Fig. 7. Conceptual framework illustrating inferred vertical organization of N uptake and transformation in a mid-depth inland water. Green and orange arrows denote nitrogen assimilation and regeneration processes, respectively. Cyn., Bac., HB, and SP represent Cyanobacteria, Bacillariophyta, Heterotrophic bacteria, and sinking particles. During stratified periods, surface NH_4^+ uptake is dominated by phytoplankton communities adapted to high light conditions and is rapidly recycled within the upper euphotic zone. Near the base of the euphotic layer, NO_3^- uptake becomes relatively more important, consistent with the presence of low-light-adapted phytoplankton. In aphotic waters, heterotrophic bacteria decompose sinking particles to release NH_4^+ while concurrently assimilating it, thereby partially decoupling N and C cycling. During the mixed period, the entire water column exhibits relatively low NH_4^+ uptake.

ambient concentration is poorly coupled to uptake due to fast biological turnover.

As a consequence, the absence of strong correlations between NH_4^+ concentration and environmental parameters does not indicate low ecological importance, but rather reflects tight biological control over its pool size. NH_4^+ uptake is therefore better interpreted as a process indicator of biological demand than as a state variable predicted by concentration alone. This decoupling explains why NO_3^-, but not NH_4^+, emerged as the variable most strongly correlated with physical gradients, even though NH_4^+ sustained the majority of nitrogen assimilation. Low ambient concentrations of urea, together with consistently low uptake rates, indicate that urea played a minor role in supporting nitrogen assimilation in this system. Rather than reflecting analytical uncertainty, the absence of a clear correlation pattern suggests that urea availability and utilization were ecologically marginal compared with NH_4^+ and NO_3^-.

Taken together, these results indicate that vertical nitrogen uptake patterns in this reservoir are governed by the combined and interacting effects of light availability, substrate concentrations, temperature, and biological community structure. While light emerges as a dominant proximal control on autotrophic uptake within the euphotic zone, especially under relatively uniform substrate conditions, other factors become increasingly important near the base of the euphotic layer and across the thermocline. In these transition zones, changes in light, nutrient availability, physicochemical conditions, and microbial composition co-occur and cannot be disentangled based on field observations alone. Therefore, the observed vertical patterns should be interpreted as emergent properties of a multifactorial system rather than responses to a single controlling variable.

4.4. *Implications for nitrogen management*

Our findings underscore the pivotal role of NH_4^+ in sustaining reservoir productivity. Due to its high bioavailability, rapid turnover, and efficient recycling, NH_4^+ supported assimilation even at low ambient concentrations, both in the euphotic and aphotic zones. This pattern challenges steady-state models and monitoring frameworks that focus solely on total N loads or bulk DIN concentrations. Instead, it highlights the necessity of distinguishing N forms when evaluating ecological risk and designing management strategies. For example, episodic NH_4^+ pulses from agricultural runoff, wastewater inputs, or atmospheric deposition might trigger immediate phytoplankton responses to stimulate bloom formation, whereas equivalent increases in NO_3^- may not.

Our results further expand the understanding of nitrogen cycling in deep and stratified reservoirs. In such ecosystems, N inputs to deeper layers, whether from sediment release, groundwater discharge, or river inflow, may initially appear ecologically irrelevant because they remain isolated from the photic zone. However, internal cycling allows NH_4^+ to accumulate and persist in hypoxic hypolimnion. When stratification is disrupted by seasonal mixing or extreme weather events (e.g., typhoons), this stored NH_4^+ can be rapidly transported into surface waters, triggering short-term nutrient enrichment and algal blooms. This "delayed response" highlights the importance of managing outlet depth in reservoirs with hypolimnetic outlets and the need to evaluate the timing and vertical location of N inputs, since their ecological impacts may only become apparent after mixing events.

Furthermore, our findings highlight the significant role of heterotrophic processes in both the euphotic and aphotic zones, which must be integrated into nutrient management frameworks. Heterotrophic bacteria contribute substantially to NH_4^+ assimilation, particularly in dark waters where NH_4^+ uptake persists despite the absence of photosynthesis. This heterotrophic activity not only accelerates NH_4^+ turnover but also facilitates the recycling of organic nitrogen, effectively maintaining a bioavailable N pool that can fuel phytoplankton growth upon mixing. Ignoring heterotrophic assimilation may lead to an underestimation of the system's capacity to retain and recycle nitrogen, particularly in stratified systems where aphotic processes are often overlooked. Therefore, management strategies should consider not only phytoplankton-driven uptake but also the heterotrophic processes that sustain NH_4^+ cycling in the dark, as these collectively influence the timing, magnitude, and form of nitrogen available for primary production.

The observed depth-resolved nitrogen uptake patterns also have implications under ongoing global change. Warming is expected to enhance biological nitrogen uptake through temperature-dependent metabolic responses. At the same time, the expansion and persistence of hypoxic conditions in deep reservoirs may promote ammonium accumulation in bottom waters by suppressing nitrification and enhancing organic matter remineralization. Subsequent mixing events could then rapidly redistribute ammonium into the euphotic zone, reinforcing internal nitrogen recycling. Together, these processes suggest that climate-driven changes in thermal structure and oxygen availability may further intensify ammonium-based nitrogen cycling in stratified reservoirs, with potential consequences for ecosystem productivity and reservoir management.

Together, these insights emphasize that effective N management in inland waters requires (1) monitoring N speciation rather than bulk concentrations alone, (2) accounting for vertical stratification and internal cycling processes, and (3) recognizing the dual roles of autotrophic and heterotrophic communities in regulating bioavailable NH_4^+.

5. Conclusion

Our study provides evidence that NH_4^+ is the dominant N source sustaining productivity in a stratified subtropical reservoir, even though NO_3^- is the most abundant form. Surface cycling of NH_4^+ is characterized by rapid turnover and strong light dependency. Substantial NH_4^+ uptake in the aphotic zone reflects heterotrophic microbial activity, revealing spatial decoupling between C and N assimilation. Furthermore, the consistent functional partitioning of N uptake, with NH_4^+ and urea in light-rich layers versus NO_3^- in deeper waters, demonstrates light-driven structuring of microbial and phytoplankton communities (Fig. 7). Future nutrient management strategies should incorporate NH_4^+ dynamics, vertical stratification, and microbial niche partitioning to effectively regulate productivity in deep and stratified reservoirs. Our findings challenge concentration-based assessments of nutrient dynamics. Future research should quantify NH_4^+ fluxes under mixing and disturbance events and evaluate management strategies that explicitly consider N form and internal cycling.

Data availability

The data that support the findings of this study is openly available in Supplementary Information.

CRediT authorship contribution statement

Moyang Li: Writing – review & editing, Writing – original draft, Visualization, Methodology, Investigation, Formal analysis, Data curation, Conceptualization. **Xiaoyu Guo:** Methodology, Investigation, Formal analysis, Data curation. **Zifu Xu:** Writing – review & editing, Investigation. **Xianhui S. Wan:** Writing – review & editing, Formal analysis. **Lianghao Ge:** Project administration, Investigation, Formal analysis. **Wenbin Zou:** Project administration, Investigation. **Jun Yang:** Writing – review & editing. **Li-Li Han:** Writing – review & editing, Formal analysis. **Min Xu:** Writing – review & editing, Funding acquisition, Formal analysis. **Shuh-Ji Kao:** Writing – review & editing, Supervision, Resources, Funding acquisition, Formal analysis, Conceptualization.

Declaration of competing interest

The authors declare that they have no known competing financial interests or personal relationships that could have appeared to influence the work reported in this paper.

Acknowledgements

We are deeply thankful to Anqi Yao, Bingchen Lyu, Sumei Li and Haowen Zhong for their help during sample collection and incubation experiments. This research was supported by the National Natural Science Foundation of China (92251306, W2411034), the Innovational Fund for Scientific and Technological Personnel of Hainan Province (KJRC2023B04) and the Ph.D. Fellowship of Xiamen University.

Supplementary materials

Supplementary material associated with this article can be found, in the online version, at doi:10.1016/j.wroa.2026.100508.

References

Baer, S.E., Sipler, R.E., Roberts, Q.N., Yager, P.L., Frischer, M.E., Bronk, D.A., 2017. Seasonal nitrogen uptake and regeneration in the western coastal Arctic. Limnol. Oceanogr. 62 (6), 2463–2479.

Braman, R.S., Hendrix, S.A., 1989. Nanogram nitrite and nitrate determination inenvironmental and biological materials by vanadium (III) reduction withchemiluminescence detection. Anal. Chem. 61 (24), 2715–2718.

Casciotti, K.L., Sigman, D.M., Hastings, M.G., Bohlke, J.K., Hilkert, A., 2002. Measurement of the oxygen isotopic composition of nitrate in seawater and freshwater using the denitrifiers method. Anal. Chem. 74 (19), 4905–4912.

Chimney, M.J., Wenkert, L., Pietro, K.C., 2006. Patterns of vertical stratification in a subtropical constructed wetland in south Florida (USA). Ecol. Eng. 27, 322–330. https://doi.org/10.1016/j.ecoleng.2006.05.017.

Deng, W., Wang, S., Wan, X., Zheng, Z., Jiao, N., Kao, S.-J., Moore, J.K., Zhang, Y., 2021. Potential competition between marine heterotrophic prokaryotes and autotrophic picoplankton for nitrogen substrates. Limnol. Oceanogr. 66 (9), 3338–3355.

Ferber, L.R., Levine, S.N., Lini, A., Livingston, G.P., 2004. Do cyanobacteria dominate in eutrophic lakes because they fix atmospheric nitrogen? Freshw. Biol. 49 (6), 690–708. https://doi.org/10.1111/j.1365-2427.2004.01218.x.

Frost, P.C., Pearce, N.J.T., Berger, S.A., Gessner, M.O., Makower, A.K., Marzetz, V., Nejstgaard, J.C., Pralle, A., Schälicke, S., Wacker, A., Wagner, N.D., Xenopoulos, M. A., 2023. Interactive effects of nitrogen and phosphorus on growth and stoichiometry of lake phytoplankton. Limnol. Oceanogr. 68 (5), 1172–1184. https://doi.org/10.1002/lno.12337.

Glibert, P.M., 2017. Eutrophication, harmful algae and biodiversity — Challenging paradigms in a world of complex nutrient changes. Mar. Pollut. Bull. 124 (2), 591–606. https://doi.org/10.1016/j.marpolbul.2017.04.027.

Glibert, P.M., Wilkerson, F.P., Dugdale, R.C., Raven, J.A., Dupont, C.L., Leavitt, P.R., Parker, A.E., Burkholder, J.M., Kana, T.M., 2016. Pluses and minuses of ammonium and nitrate uptake and assimilation by phytoplankton and implications for productivity and community composition, with emphasis on nitrogen-enriched conditions. Limnol. Oceanogr. 61 (1), 165–197. https://doi.org/10.1002/lno.10203.

Glibert, P.M., Maranger, R., Sobota, D.J., Bouwman, L., 2014. The Haber Bosch–harmful algal bloom (HB–HAB) link. Environ. Res. Lett. 9 (10), 105001.

Gu, B., Alexander, V., 1993. Dissolved nitrogen uptake by a cyanobacterial bloom (Anabaena flos-aquae) in a subarctic lake. Appl. Environ. Microbiol. 59 (2), 422–430. https://doi.org/10.1128/aem.59.2.422-430.1993.

Henderson, L.C., English, C.J., Jeng, D.L., Popendorf, K.J., Carlson, C.A., Close, H.G., 2025. Carbohydrate content controls vertical variations in carbon to nitrogen ratios of organic particles within the euphotic zone in the northwest Sargasso Sea. Commun. Earth Environ. 6 (1), 547. https://doi.org/10.1038/s43247-025-02524-6.

Joint, I., Henriksen, P., Fonnes, G.A., Bourne, D., Thingstad, T.F., Riemann, B., 2002. Competition for inorganic nutrients between phytoplankton and bacterioplankton in nutrient manipulated mesocosms. Aquat. Microbial Ecol. 29 (2), 145–159.

Kao, S.-J., Terence Yang, J.-Y., Liu, K.-K., Dai, M., Chou, W.-C., Lin, H.-L., Ren, H., 2012. Isotope constraints on particulate nitrogen source and dynamics in the upper water column of the oligotrophic South China Sea. Glob. Biogeochem. Cycles 26 (2). https://doi.org/10.1029/2011GB004091.

Knapp, A.N., Sigman, D.M., Lipschultz, F., 2005. N isotopic composition of dissolved organic nitrogen and nitrate at the Bermuda Atlantic Time-series Study site. Glob. Biogeochem. Cycles 19 (1). https://doi.org/10.1029/2004GB002320.

Kumar, S., Sterner, R.W., Finlay, J.C., 2008. Nitrogen and carbon uptake dynamics in Lake Superior. J. Geophys. Res.: Biogeosci. 113 (G4). https://doi.org/10.1029/2008jg000720.

Levine, S.N., Shambaugh, A.d., Pomeroy, S.E., Braner, M., 1997. Phosphorus, nitrogen, and silica as controls on phytoplankton biomass and species composition in Lake Champlain (USA-Canada). J. Great Lakes Res. 23 (2), 131–148. https://doi.org/10.1016/S0380-1330(97)70891-8.

Lehmann, M.F., Bernasconi, S.M., McKenzie, J.A., Barbieri, A., Simona, M., Veronesi, M., 2004. Seasonal variation of the δ_c and δ_n of particulate and dissolved carbon and nitrogen in Lake Lugano: constraints on biogeochemical cycling in a eutrophic lake. Limnol. Oceanogr. 49 (2), 415–429. https://doi.org/10.4319/lo.2004.49.2.0415.

Liu, L., Chen, H., Liu, M., Yang, J.R., Xiao, P., Wilkinson, D.M., Yang, J., 2019. Response of the eukaryotic plankton community to the cyanobacterial biomass cycle over 6 years in two subtropical reservoirs. ISME J. 13 (9), 2196–2208. https://doi.org/10.1038/s41396-019-0417-9.

Li, S., Yan, X., Chen, H., Jeppesen, E., Xiao, P., Jin, L., Xu, Z., Zuo, J., Ren, K., Yang, J., 2025. Cyanobacterial blooms specifically alter the dispersal-mediated taxonomic and functional vertical similarity of microbial communities in a subtropical reservoir. Water Res. 281, 123574. https://doi.org/10.1016/j.watres.2025.123574.

Mendonça, R., Müller, R.A., Clow, D., Verpoorter, C., Raymond, P., Tranvik, L.J., Sobek, S., 2017. Organic carbon burial in global lakes and reservoirs. Nat. Commun. 8 (1), 1694. https://doi.org/10.1038/s41467-017-01789-6.

Paerl, H.W., Scott, J.T., McCarthy, M.J., Newell, S.E., Gardner, W.S., Havens, K.E., Hoffman, D.K., Wilhelm, S.W., Wurtsbaugh, W.A., 2016. It takes two to tango: when and where dual nutrient (N & P) reductions are needed to protect lakes and downstream ecosystems. Environ. Sci. Technol. 50 (20), 10805–10813. https://doi.org/10.1021/acs.est.6b02575.

Présing, M., Herodek, S., Preston, T., Vörös, L., 2001. Nitrogen uptake and the importance of internal nitrogen loading in Lake Balaton. Freshw. Biol. 46 (1), 125–139. https://doi.org/10.1111/j.1365-2427.2001.00622.x.

RAVEN, J.A., WOLLENWEBER, B., HANDLEY, L.L., 1992. A comparison of ammonium and nitrate as nitrogen sources for photolithotrophs. New Phytolog. 121 (1), 19–32. https://doi.org/10.1111/j.1469-8137.1992.tb01088.x.

Revilla, M., Alexander, J., Glibert, P.M., 2005. Urea analysis in coastal waters: comparison of enzymatic and direct methods. Limnol. Oceanography: Methods 3 (7), 290–299. https://doi.org/10.4319/lom.2005.3.290.

Salk, K.R., Bullerjahn, G.S., McKay, R.M.L., Chaffin, J.D., Ostrom, N.E., 2018. Nitrogen cycling in Sandusky Bay, Lake Erie: oscillations between strong and weak export and implications for harmful algal blooms. Biogeosciences 15 (9), 2891–2907. https://doi.org/10.5194/bg-15-2891-2018.

Scavia, D., David Allan, J., Arend, K.K., Bartell, S., Beletsky, D., Bosch, N.S., Brandt, S.B., Briland, R.D., Daloğlu, I., DePinto, J.V., Dolan, D.M., Evans, M.A., Farmer, T.M., Goto, D., Han, H., Höök, T.O., Knight, R., Ludsin, S.A., Mason, D., …Zhou, Y., 2014. Assessing and addressing the re-eutrophication of Lake Erie: central basin hypoxia. J. Great Lakes Res. 40 (2), 226–246. https://doi.org/10.1016/j.jglr.2014.02.004.

Sepp, M., Tamm, M., Newell, S.E., Myers, J.A., Hunt, T., Palmik-Das, K., Tuvikene, L., Nõges, P., Nõges, T., McCarthy, M.J., 2025. Water column ammonium regeneration supports productivity in two large, eutrophic lakes. Limnol. Oceanogr. https://doi.org/10.1002/lno.70047.

Wan, X.S., Sheng, H.X., Dai, M., Zhang, Y., Shi, D., Trull, T.W., Zhu, Y., Lomas, M.W., Kao, S.J., 2018. Ambient nitrate switches the ammonium consumption pathway in the euphotic ocean. Nat Commun 9 (1), 915. https://doi.org/10.1038/s41467-018-03363-0.

Sigman, D.M., Casciotti, K.L., Andreani, M., Barford, C., Galanter, M.B.J.K., Bohlke, J.K., 2001. A bacterial method for the nitrogen isotopic analysis of nitrate in seawater and freshwater. Anal. Chem. 73 (17), 4145–4153.

Wan, X.H.S., Sheng, H.X., Dai, M.H., Church, M.J., Zou, W.B., Li, X.L., Hutchins, D.A., Ward, B.B., Kao, S.J., 2021. Phytoplankton-nitrifier interactions control the geographic distribution of nitrite in the Upper ocean. Glob. Biogeochem. Cycles 35 (11).

Wu, Z., Yu, D., Yu, Q., Liu, Q., Zhang, M., Dahlgren, R.A., Middelburg, J.J., Qu, L., Li, Q., Guo, W., Chen, N., 2024. Greenhouse gas emissions (CO_2–CH_4–N_2O) along a large reservoir-downstream river continuum: the role of seasonal hypoxia. Limnol. Oceanogr. 69, 1015–1029. https://doi.org/10.1002/lno.12544.

Wheeler, P.A., Kirchman, D.L., 1986. Utilization of inorganic and organic nitrogen by bacteria in marine systems. Limnol. Oceanogr. 31 (5), 998–1009.

Xu, M.N., Li, X.L., Shi, D.L., Zhang, Y., Dai, M.H., Huang, T., Glibert, P.M., Kao, S.J., 2019. Coupled effect of substrate and light on assimilation and oxidation of regenerated nitrogen in the euphotic ocean. Limnol. Oceanogr. 64 (3), 1270–1283. https://doi.org/10.1002/lno.11114.

Xue, Q., Xie, L., Yang, J.R., Yang, J., Su, X., 2024. The prevalence and persistence of microcystin in seven subtropical reservoirs in China and associated potential risks for human health. Environ. Technol. Innov. 33, 103476. https://doi.org/10.1016/j.eti.2023.103476.

Yang, J., Lv, H., Yang, J., Liu, L., Yu, X., Chen, H., 2016. Decline in water level boosts cyanobacteria dominance in subtropical reservoirs. Sci. Total Environ. 557-558, 445–452. https://doi.org/10.1016/j.scitotenv.2016.03.094.

Yang, J.R., Lv, H., Isabwe, A., Liu, L., Yu, X., Chen, H., Yang, J., 2017. Disturbance-induced phytoplankton regime shifts and recovery of cyanobacteria dominance in two subtropical reservoirs. Water Res. 120, 52–63. https://doi.org/10.1016/j.watres.2017.04.062.

Zhang, S., Arhonditsis, G.B., Ji, Y., Bryan, B.A., Peng, J., Zhang, Y., Gao, J., Zhang, J., Cho, K.H., Huang, J., 2025. Climate change promotes harmful algal blooms in China's lakes and reservoirs despite significant nutrient control efforts. Water Res. 277, 123307. https://doi.org/10.1016/j.watres.2025.123307.